GENESIS OF AN ARCHAEAN QUARTZ-FELDSPAR PORPHYRY

A thesis submitted to the Department of Geology in partial fulfillment of the requirements for the degree Bachelor of Sciences

Bachelor of Sciences (1985) McMaster University
(Geology) Hamilton, Ontario

TITLE: GENESIS OF AN ARCHAEAN QUARTZ-FELDSPAR PORPHYRY

AUTHOR: Ian S. Cooper

SUPERVISOR: Dr. R. H. McNutt

NUMBER OF PAGES: 43 , v

SCOPE OF CONTENTS:

Three conformable units of fine-grained quartz-feldspar porphyry were mapped in the Berry River Formation, Warclub Group, Northwestern Ontario. The largest unit (Unit 1) is compared geochemically and petrographically to quartz-feldspar porphyry intrusions and tuffs in the area with the aim of determining the method of emplacement of the porphyry unit (Unit 1), and consequently the other two units.

ACKNOWLEDGEMENTS

I would like to thank the Ontario Geological Survey for allowing time for data collection. I would especially like to thank Mr. G. Johns of the OGS for his aid in the production of this thesis, and for his interesting correspondences (ONGYS). Some of the mapping was done by Mr. G. Johns and Mr. J. Davison.

I would like to express my gratitude to Dr. R. H. McNutt for his instruction and supervision of this thesis.

O. Mudrock aided in the preparation and analysis of samples by XRF. L. Zwicker aided in the preparation of thin sections. J. Whorwood prepared the photoraphic plates.

Finally, special thanks to Miss W. Mertick, who believed in me, and also to the geology students at Mac, especially the graduating class of 1985, for making the past four years bearable.

"Obscurum per obscurius"...

TABLE OF CONTENTS

LIST OF FIGURES

CHAPTER ONE:

INTRODUCTION AND GENERAL GEOLOGY

1.1 Location and Access

The map area for this study is approximately 9 km^2, bounded roughly by Latitudes 49°26'00" N and 49°27'00" N and by Longitudes 93°58'30" W and 94° 01'00" W. The village of Sioux Narrows is 10 km to the south on Highway 71 (see location map, Fig. 1.1); the Town of Kenora lies 50 km to the northwest.

Access to the area east of Highway 71 is via the Maybrun Road, an Ontario Ministry of Natural Resources Forest Access Road, from Highway 71 itself, as well as by canoe from Long Bay, Lake of the Woods. The thesis area is contained by the Maybrun Road and Berry Lake to the north; by the Berry River to the east; by Robert's Road to the south and by Long Bay to the west.

Outcrop exposure is roughly 10%.

1.2 Method and Purpose of Study

The field area was mapped over a period of seven days during July and August, 1984. Preliminary traverses were completed before detailed mapping and sampling were undertaken at selected points.

Three stratigraphically sequential units of fine-grained, felsic, porphyritic rock were the main subject of interest. They all conform to regional strike but show no clear contact relationships with the surround-

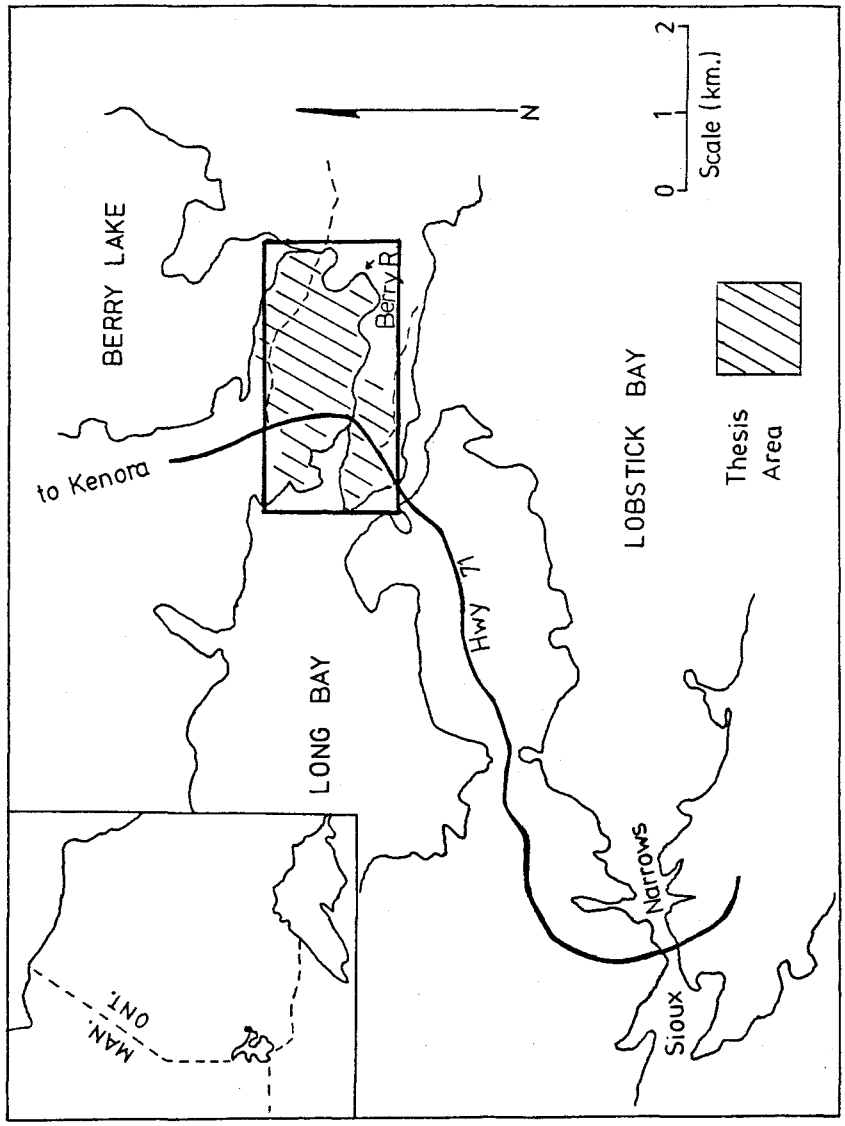

Figure 1.1 Thesis area (shaded) location map.

ing pyroclastic sequences. They have similarities with both the crystal tuffs and intrusive porphyries found in the region.

These three porphyritic units have been interpreted as ash-flow tuffs in a facies model proposed for the region (Johns, in prep.). However, no detailed work has been done to establish whether or not these porphyritic units are ash flow deposits.

The purpose of this paper is to establish the genesis of these porphyritic units. Three possible methods of emplacement are considered:

(i) ash flow

(ii) intrusion

(iii) lava flow.

To achieve this, a map of the field area was produced (see Figure 1.2.1) followed by laboratory studies in geochemistry and petrography.

It was necessary to establish the field relationships between the porphyries and the neighbouring pyroclastics (it should be noted here that the term "porphyry" is used thoughout this paper to indicate a texture alone--there is no genetic connotation in the use of this term). Therefore, field studies were concentrated at the contacts to determine their nature --conformable; intrusive (baked or chilled margins); gradational with pyroclastic sequences; erosive, etc.

Representative hand samples were collected from

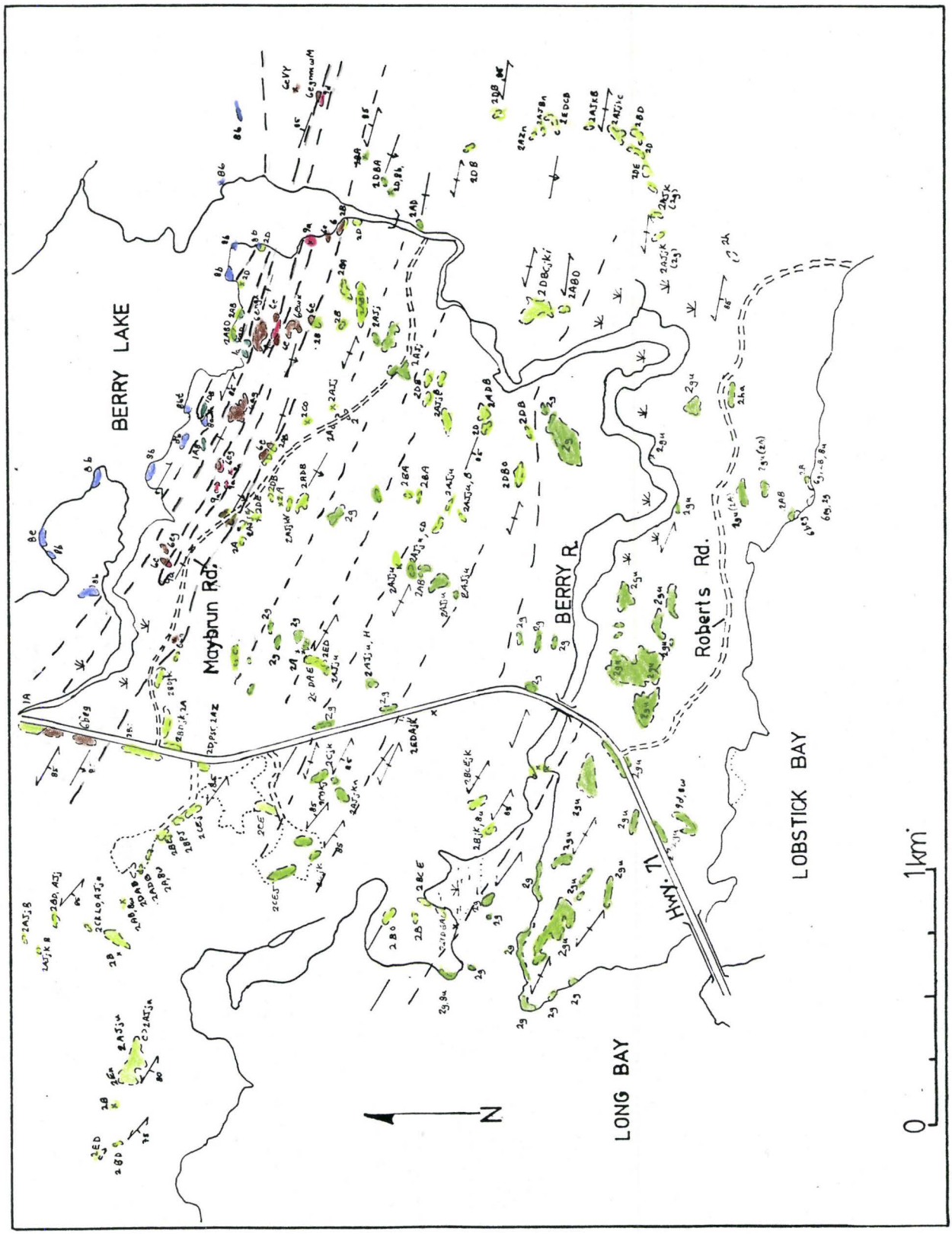

Figure 1.2.1 Thesis area outcrop data. 1=mafic metavolcanics, 2=intermediate to felsic metavolcanics, 6=clastic metasediments, 8=mafic intrusive, 9= metamorphosed porphyry intrusion. Some data from Johns (1983a,b)

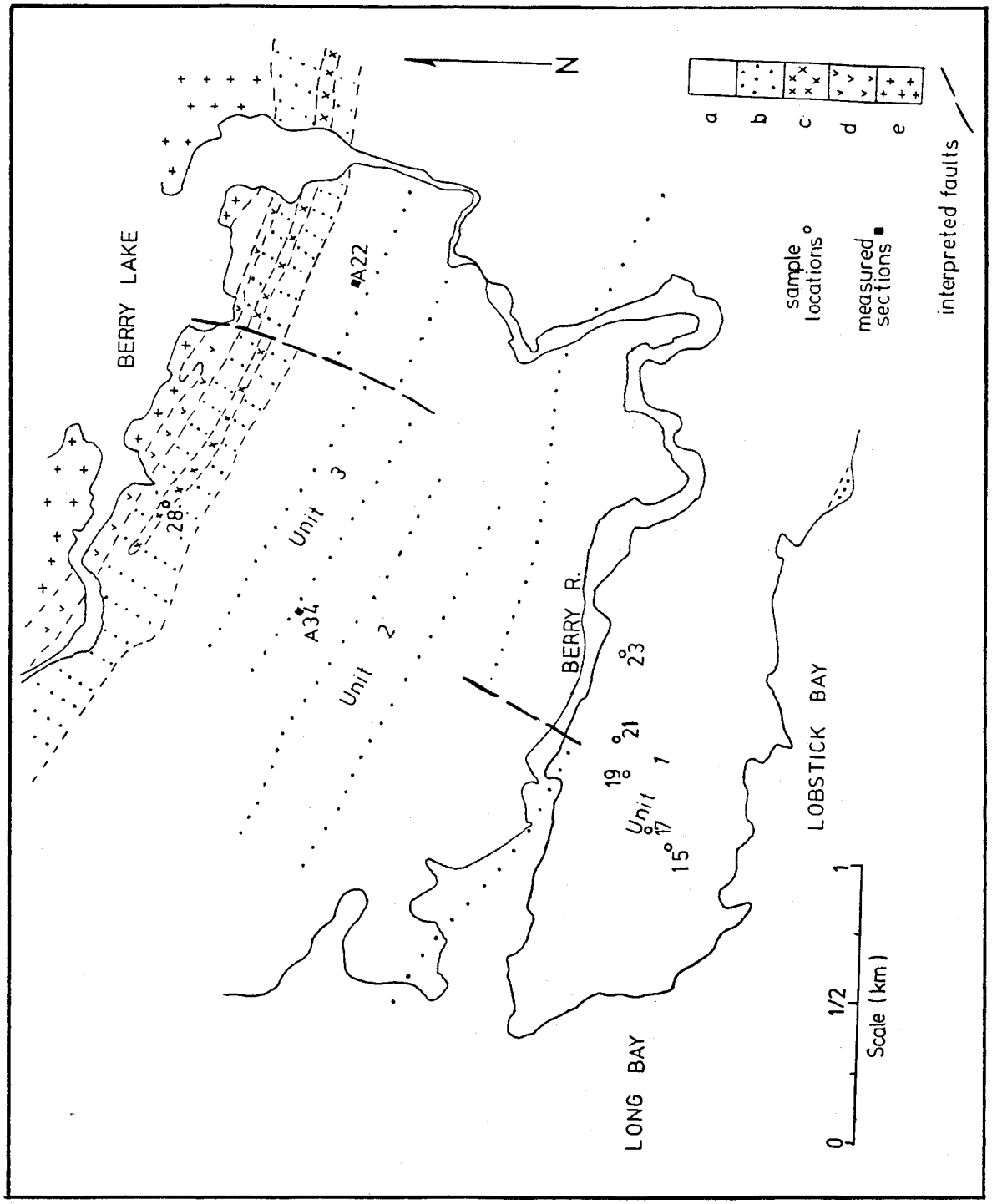

Figure 1.2.2 Interpretation of Figure 1.2.1, showing geochemistry sample locations and measured section locations. a=intermediate to felsic metavolcanics; b=clastic metasediments; c=metamorphosed porphyry intrusion; d=mafic metavolcanics; e=metamorphosed mafic intrusion (gabbro).

the metavolcanics and porphyries for thin section. As well, samples for geochemistry were collected at regular intervals (every 65 m) in a traverse perpendicular to strike across the largest porphyritic unit (Unit 1 in Figure 1.2.2). This procedure was followed to determine whether there are any systematic variations across strike in the units not visible on outcrop scale. Unit 1 was chosen as being the most likely to show variation because of its size. Due to the similarity between the three porphyry units, it was assumed that conclusions drawn for Unit 1 would be equally applicable to the other two units.

Samples also were collected from two intrusive quartz-feldspar porphyries in and around the map area for petrographic and geochemical comparison with the porphyries under study.

Hand samples from all porphyries are very dense.

1.3 Regional Geology

The geology of the region is summarised from Stockwell (1970), and Trowell, et al. (1980).

The map area is situated in the northwest portion of the Savant Lake—Crow Lake Belt in the Wabigoon Subprovince of the Archaean Superior Province (see Figure 1.3).

The Wabigoon Belt is characterised by arcuate supracrustal volcano-sedimentary sequences deformed by younger batholithic intrusions. These volcanics and sediments were metamorphosed, faulted, folded and in-

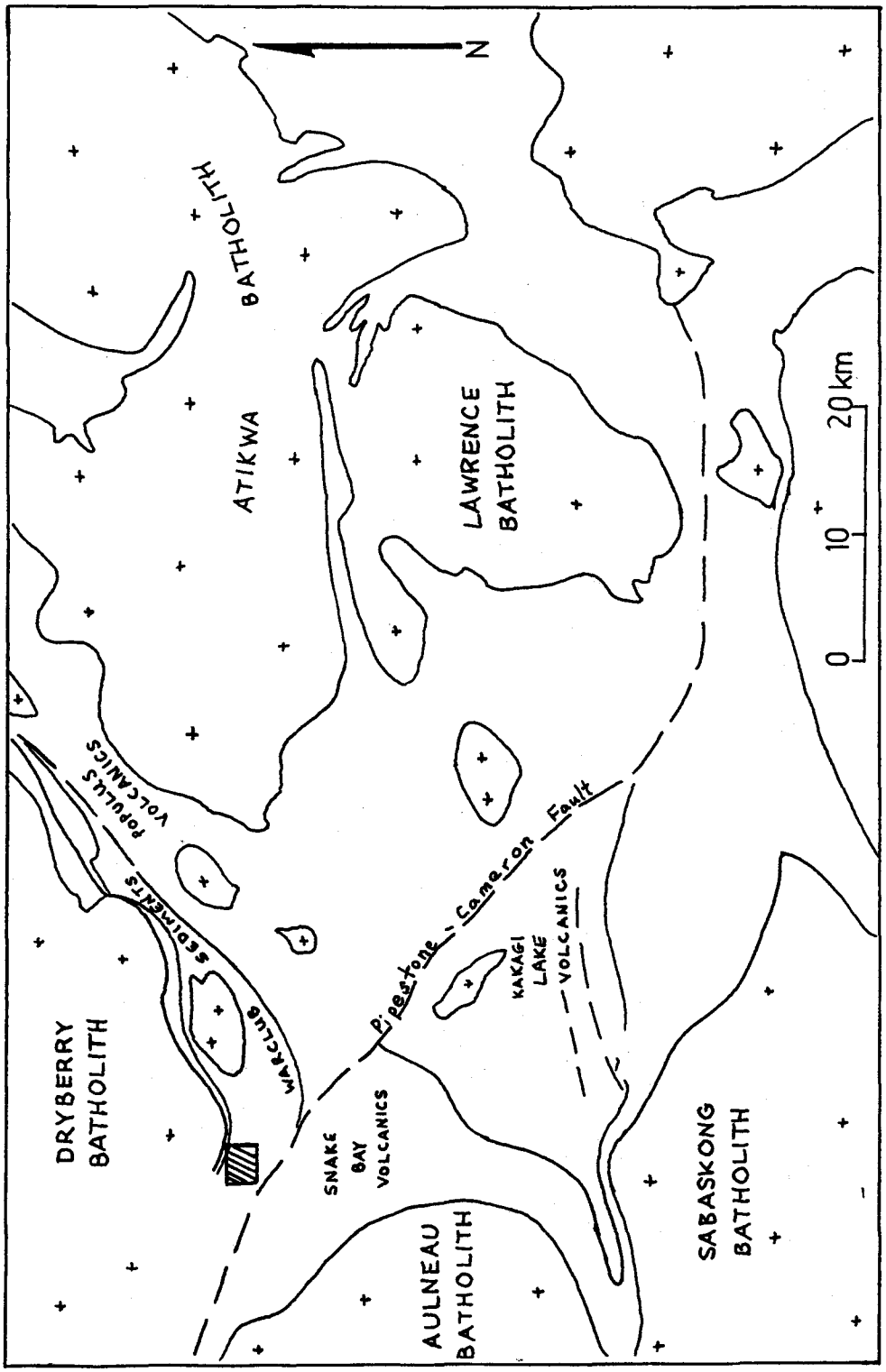

Figure 1.3 A portion of the Savant Lake-Crow Lake Belt, NW Ontario. Figure simplified from Trowell, et al. (1980). Thesis area shaded.

truded by granitic rocks during the Kenoran Orogeny. Major shear zones, such as the Pipestone-Cameron Fault (see Figure 1.3) may be late-stage effects of this orogeny. In most areas, the volcanics are older and are overlain by the sediments, but in some areas (such as this map area) the sediments occur at the base of the exposed sequence (implying more than one volcano-sedimentary cycle). Volcanics often grade along strike into sediments.

Maximum thicknesses in the Wabigoon Subprovince vary from belt to belt, and within individual belts, ranging up to 15 000 m. The thickness of the volcano-sedimentary sequence near the map area has been estimated at 8200 m by Moorhouse (1965). Volcanic rocks comprise the majority of the thicker successions, dominated by basalts, with lesser amounts of intermediate to felsic lavas, tuffs and breccias. The intermediate to felsic portions tend to occur locally as thick sequences. Felsic, porphyritic, fine-grained hypabyssals commonly occur in or near the volcanics, and may be contemporaneous with volcanic activity.

1.4 Geology of the Warclub Group

The area was previously mapped by Burwash (1934) as part of a survey covering a larger area. Johns (1983a, 1983b) completed quarter-mile mapping of the

Long Bay—Lobstick Bay area, including the area of interest, during the 1982 and 1983 field seasons.

All rocks exposed in the area are of Archaean age. Davis and Edwards (1982) have dated a quartz-feldspar porphyry in the Berry River Formation (see Figure 1.4) by the U-Pb zircon method at 2714 million years.

Two differing geologic environments are divided by the Pipestone-Cameron Fault (see Figure 1.4). The predominantly mafic Snake Bay Formation lies to the south of the fault, the intermediate to felsic Berry River Formation to the north. The greenschist facies metamorphic rocks of the Berry River Formation south of Berry Lake to the fault form a south-facing homoclinal sequence of predominantly pyroclastics and quartz-feldspar porphyry.

Shoreline outcrops on Berry Lake consist mainly of metamorphosed gabbro to melanogabbro (unit 'e' on Fig. 1.2.2) of the Point Bay Group, with local shearing. This intrudes an eastward-thinning unit of mafic tuffs, lapilli tuffs and tuff breccias of the Warclub Group (unit 'd'). In the northeast corner of the map area there is a small remnant package of intermediate pyroclastics that lies stratigraphically below these mafics. Overlying the mafic unit is a 200 m thick sequence of southward-facing clastic metasediments, predominantly well-bedded feldspathic slates/argillites (unit 'b'). These sediments are intruded by a quartz-feldspar porphyry dyke about 60 m wide trending 110°—

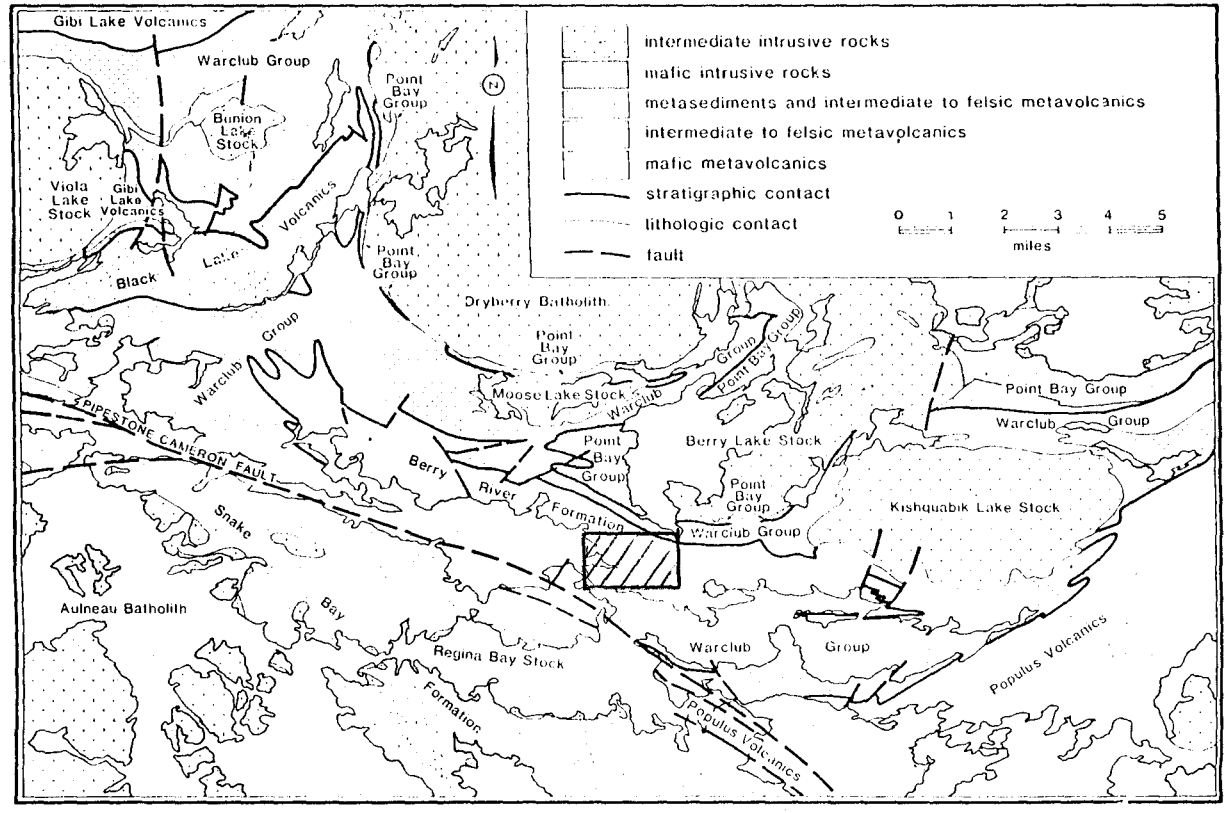

Figure 1.4 Stratigraphic map of region surrounding thesis area. Figure from Johns (1983b). Thesis area shaded.

120° (unit 'c').

Overlying the sediments with slight unconformity and comprising the greater part of the map area is a thick sequence of intermediate to felsic metavolcanics, mostly pyroclastics. This is the Berry River Formation of the Warclub Group.

1.5 Structural Geology

The Berry River Formation strikes 110°—120° and tops uniformly to the south. The thesis area lies just to the north (about 1.5 km.) of the regional northwest-southeast Pipestone-Cameron Fault. Consequently the rocks are intensely sheared and altered throughout the map area (Blackburn, 1981). Shearing appears to be bedding-plane parallel overall, as seen in the elongation of pyroclasts parallel to bedding surfaces. Measurements of maximum, minimum and average pyroclast size give elongation ratios from 5:1 to 10:1. It was assumed that the intensity of shearing would increase closer to the fault, however, no consistent relationship was found between degree of elongation and proximity to the Pipestone-Cameron Fault.

CHAPTER TWO:

GEOLOGY OF THE BERRY RIVER FORMATION

2.1 Porphyries

Field work was concentrated in the contact areas between the porphyries (described in Section 1.2) and neighbouring pyroclastics. Despite detailed outcrop-scale mapping and outcrop cleaning, no actual contacts were observed due to the poor exposure. Porphyry outcrops within 10 m of definite pyroclastic outcrops showed no boundary-controlled changes in grain size or degree of phenocryst crystallinity. Nothing which could be interpreted as baked or chilled margins was observed upon passing from pyroclastic outcrops to porphyry outcrops.

The lowest porphyry (Unit 3 on Figure 1.2.2) is about 200 m thick and can be traced for approximately 2 km along strike. The middle porphyry (Unit 2) is about 300 m. thick and extends beyond the western edge of the map area, but can only be traced to within 500 m of the Berry River to the east. The upper porphyry is at least 600 m thick, although it may be thicker due to faulting, and it extends beyond both the east and west perimeters.

The three units are all similar, characterised by 0.1—1.0 cm quartz and feldspar phenocrysts in a fine-grained siliceous matrix (see Plate 2.1.). Phenocrysts vary in size, abundance and proportion across

PLATE 2.1

(A) Porphyry Unit 1 outcrop -- note abundant feldspar and quartz phenocrysts.

(B) Localised 'clasts' or shearing within the porphyry Unit 1.


CENTIMETRE
A

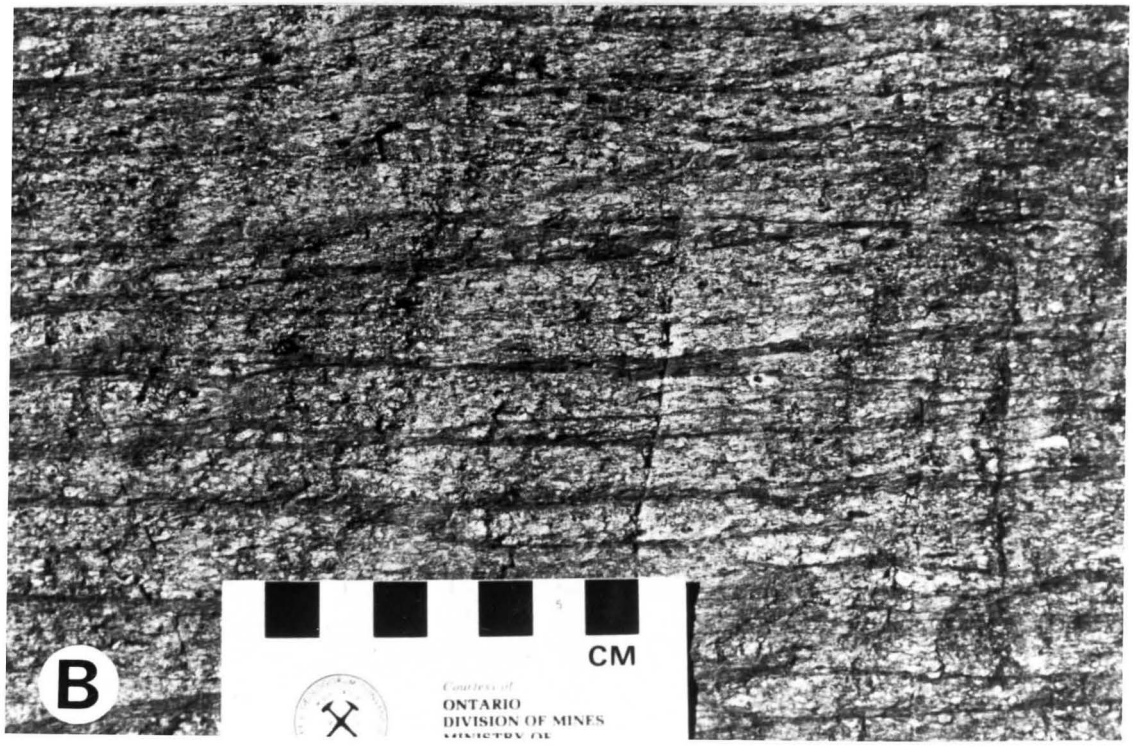
CM
B
Courtesy of
ONTARIO
DIVISION OF MINES

strike, but in no systematic manner (i.e., unrelated to position within the mappable unit). The phenocrysts average between 0.1 and 0.3 cm , and may comprise up to 20—25% of the rock, but average around 10—15%. Quartz/feldspar ratios may be as low as 1/1 but ratios of 1/2 or 1/3 are more common. Some feldspars appeared crudely aligned at two locations. Blue quartz eyes are a common constituent, some being found in almost all samples.

Some localised spots appear to contain lensoidal clasts of highly variable size (see Plate 2.1). These are very subtle features and it is not known whether they are due to tectonism ('anastomosing shear planes') or represent actual clast-rich horizons.

Calcite may be present in veins or along fractures, especially in those areas closer to the Pipestone-Cameron Fault.

2.2 Pyroclastics

The pyroclastic terminology used in this section is presented in Figure 2.2.1.

Volcanic rocks in the area are predominantly interbedded felsic to intermediate, fine to coarse homolithic pyroclastics. The commonest rock types are tuff (>80% ash), lapilli tuff (tuff and lapilli fragments), and tuff breccia (lapilli, blocks and tuff--see Plate 2.2). There are rare amounts of lapillistone (>80% lapilli) and

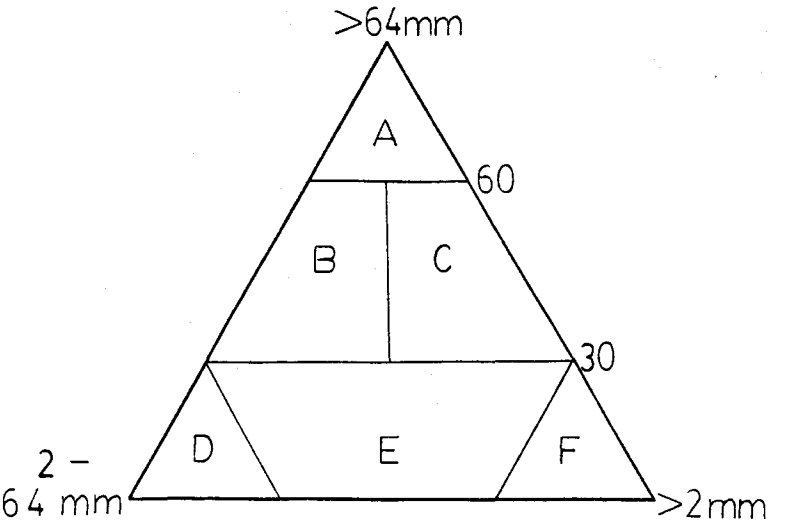

(a)

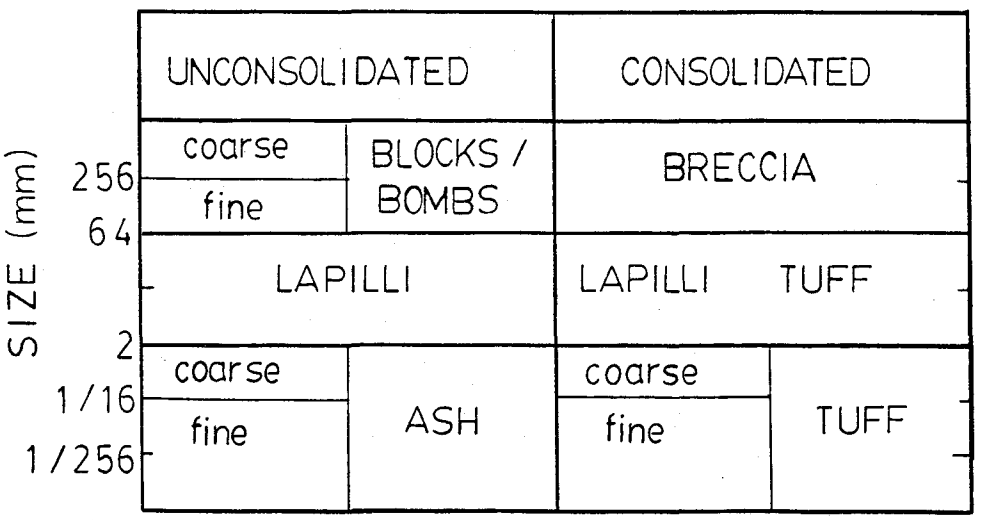

(b)

Figure 2.2.1 Pyroclastic terminology used in the text.
(a) from Easton and Johns (in prep), adapted from Schmid (1981) and Fisher (1966). A=breccia, B= lapilli tuff, C=ash-tuff breccia, D=lapilli tuff, E=lapilli-ash tuff, F=tuff.
(b) from Easton and Johns (in prep).

PLATE 2.2

(A) and (B) Tuff breccia near base of measured section A34. Note elongation of clasts. Hammer handle points north.

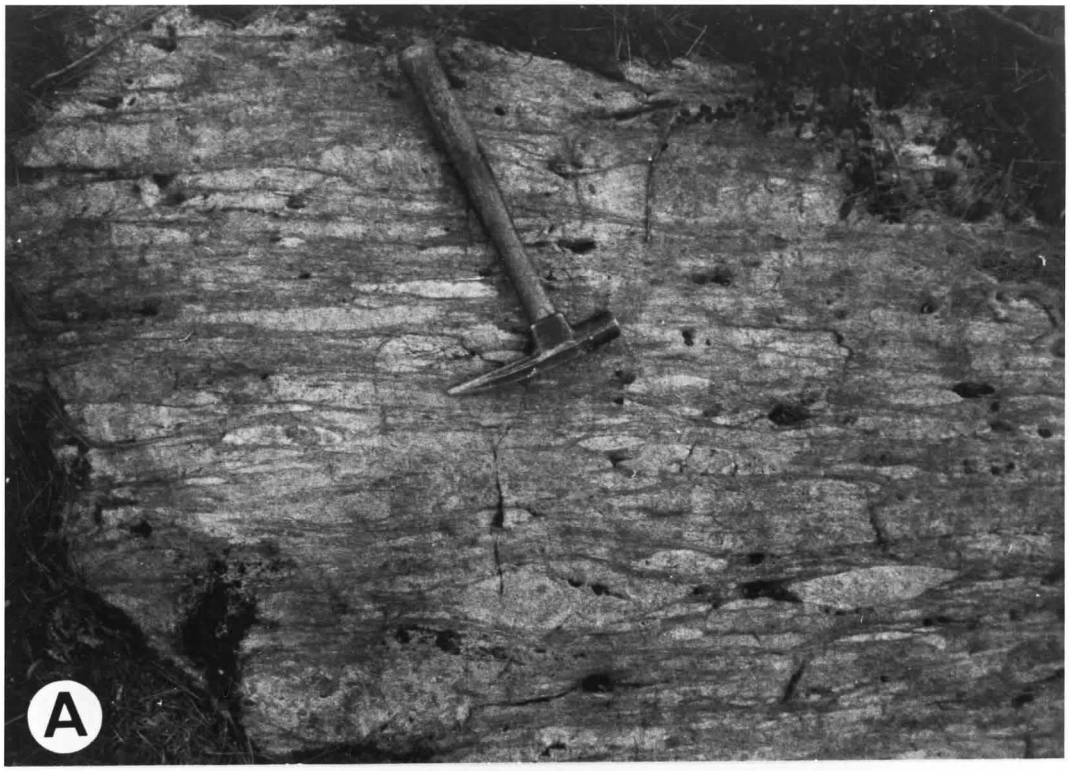
A

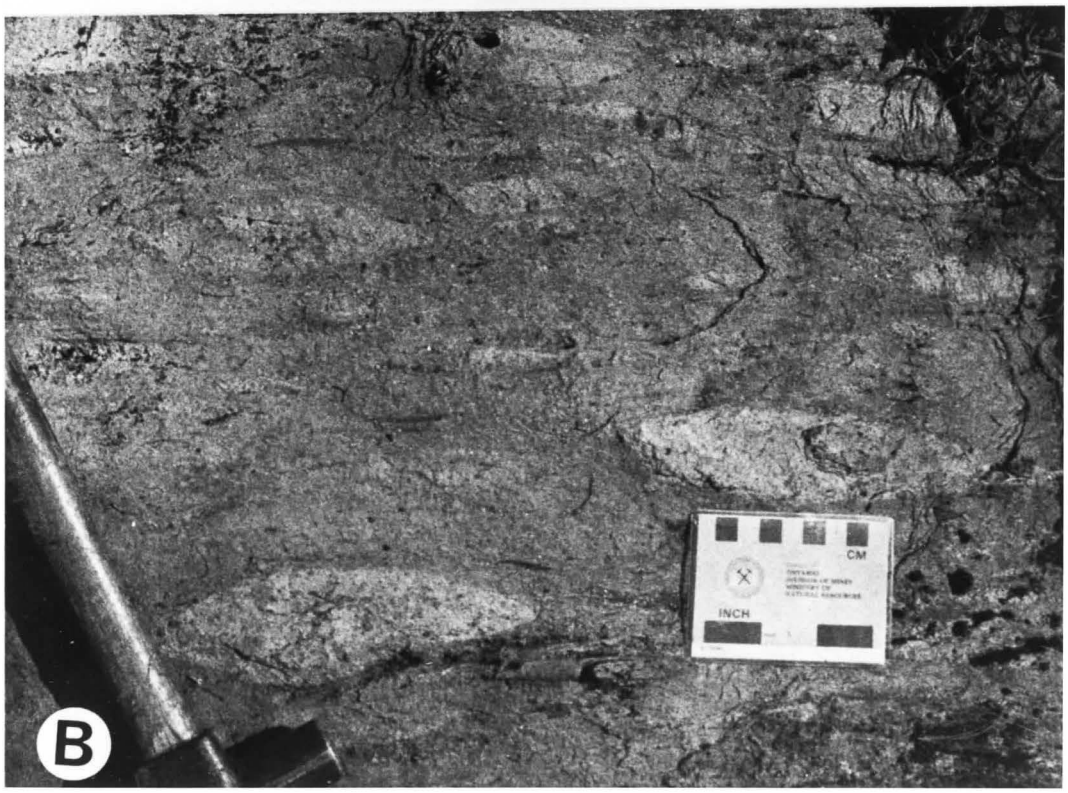
CM
INCH
B

pyroclastic breccia (>80% blocks).

There is some grading within the coarser units. The clasts are most often subround to subangular (lens-shaped). The majority of the breccias and tuffs contain clasts of quartz-feldspar porphyry, consisting of medium-grained feldspar and (blue) quartz phenocrysts (in a ratio of 3/1) set in a fine-grained siliceous matrix. These clasts are very similar to the porphyries described in the previous section. The clasts themselves are set in a fine-grained (<1 mm) quartz-feldspar tuff matrix.

Some breccias are heterolithic, containing minor amounts of lapilli-sized, medium-grained mafic clasts. This same mafic material was seen as the matrix to quartz-feldspar porphyry clasts in one mafic tuff breccia.

Sections were measured through two particularly good exposures of pyroclastics (Figures 2.2.2 and 2.2.3) adjacent to the lower porphyry (see Figure 1.2.2) while attempting to determine contact relationships. Loss of exposure prevented observation of any contacts.

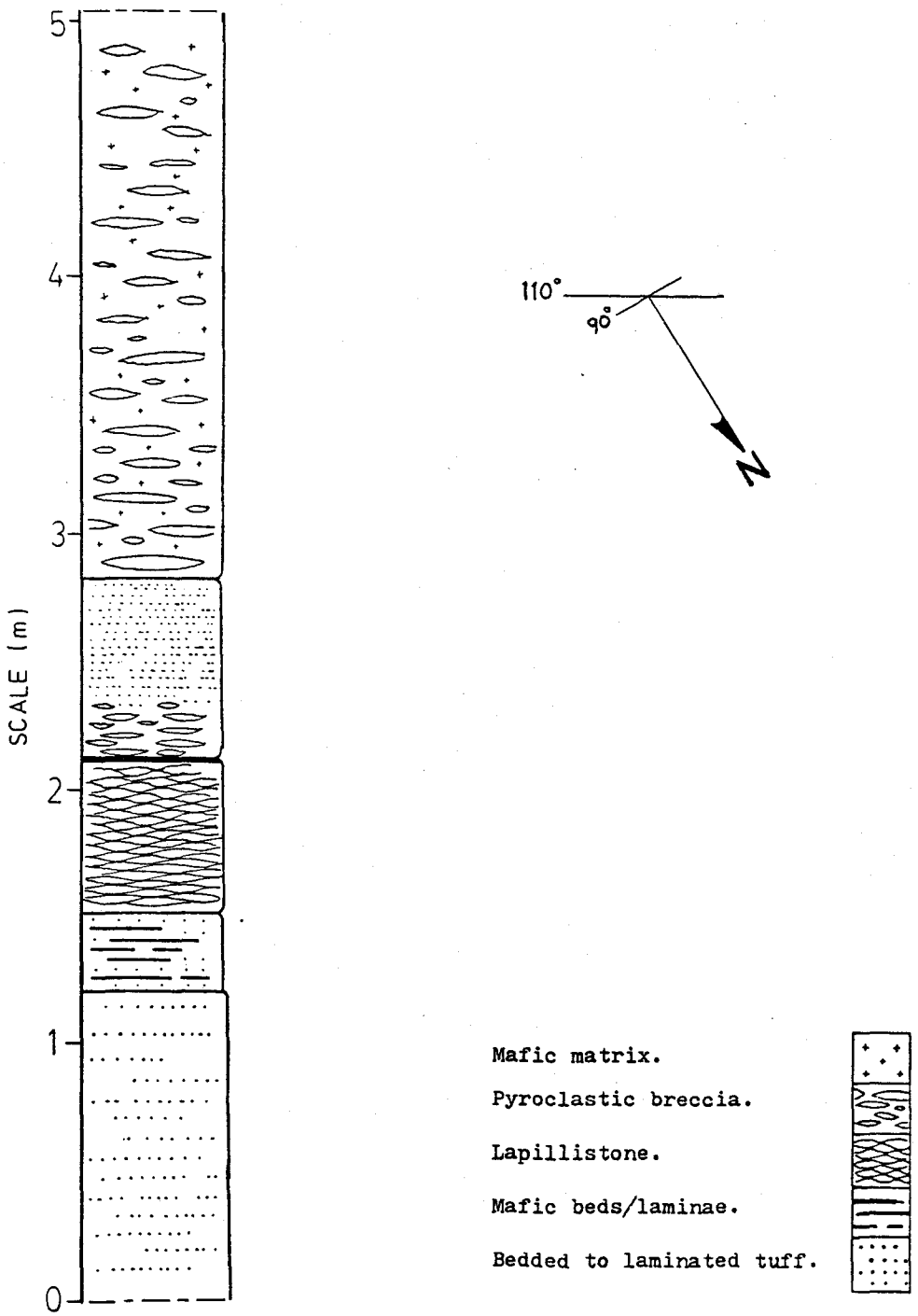

Figure 2.2.2(a) Measured section A34 through pyroclastics.

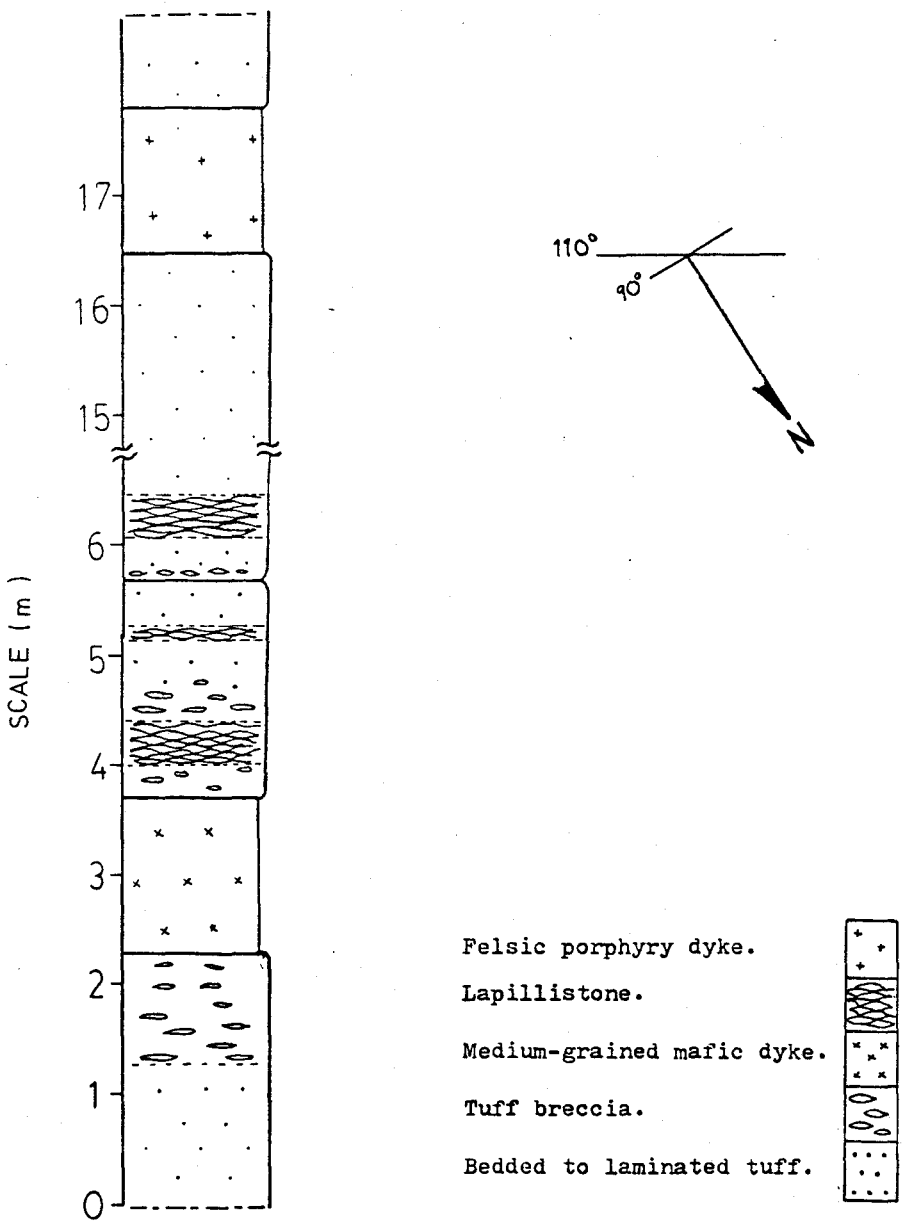

Figure 2.2.2(b) Measured section A22 through pyroclastics.

CHAPTER THREE:

GEOCHEMISTRY

3.1 Analytical Procedures

Whole rock major and trace element analyses for six samples were made using a Philips Model 1450 AHP, automatic, sequential X-ray fluorescence spectrometer within the Department of Geology at McMaster University.

Care was taken to remove all weathered surfaces prior to crushing. Samples were crushed using a Spex Industries shatter-box with tungsten-carbide rings.

A 1:1 mix of anhydrous lithium tetraborate and lithium metaborate flux was mixed with the rock powder in a ratio of 6:1 (3.0000 g of flux to 0.5000 g of sample). This mixture was fused at approximately 1200°C for three to five minutes in Pt-Au crucibles, and then was carefully poured into Pt-Au molds and cooled. These fusion pellets were analysed for the major elements Si, Al, total Fe, Mg, Ca, Na, K, Ti, Mn, and P.

Pressed powder pellets were made following a procedure modified from Marchand (1973). These pellets were analysed for the trace elements Ba, Rb, Sr, Y, Zr, and Nb.

Total loss on ignition (LOI) (CO_2 and H_2O) at 1040°C for these samples was between 2 and 4.5%.

Results of all chemical analyses are provided in Table 3.1.1.

Table 3.1.1 XRF analysis results. Major oxides listed as weight % (normalised to 100.00%). Trace elements listed in ppm. See text for explanation of 17*. 15-23=porphyry Unit 1; 28=porphyry intrusion.

	15	17*	19	21	23	28
SiO_2	69.47	69.39	70.01	70.83	70.07	71.49
Al_2O_3	16.18	15.99	16.55	15.79	16.50	16.04
Fe_2O_{3T}	2.84	2.81	2.47	2.24	3.01	2.30
MgO	0.06	0.68	0.68	0.78	0.82	0.47
CaO	4.63	4.00	2.73	2.43	1.41	2.82
Na_2O	3.08	4.23	3.38	3.51	4.82	4.56
K_2O	3.23	2.48	3.71	4.00	2.89	1.91
TiO_2	0.30	0.29	0.30	0.25	0.31	0.29
MnO	0.06	0.05	0.02	0.02	0.01	0.01
P_2O_5	0.14	0.13	0.15	0.15	0.17	0.10
LOI	4.51	2.65	3.09	2.83	2.12	2.61
Ba	908	690	237	677	680	936
Rb	61	40	62	69	47	38
Sr	439	598	378	402	301	674
Y	29	29	32	24	26	22
Zr	175	170	170	162	164	189
Nb	18	17	20	18	19	12

Table 3.1.1 (continued) Calculation of Fe_2O_3 and FeO from XRF data for Fe_2O_{3T}, for Barth norm calculations.

$$Fe_2O_3 = TiO_2 + 1.5$$

$$FeO = (Fe_2O_{3T} - Fe_2O_3)\ \frac{Fe_2O_2}{Fe_2O_3}$$

For example, calculations for sample #15:

$$Fe_2O_3 = 0.30 + 1.5$$
$$= 1.80$$

$$FeO = (2.84 - 1.80)\ 0.9$$
$$= 0.94$$

Similarly,	Fe_2O_3	FeO
17	1.79	0.92
19	1.80	0.60
21	1.75	0.44
23	1.81	1.08
28	1.79	0.46

Table 3.1.2 Calculation of average value and error from triplicate sample. Major oxides listed in weight %. Trace elements listed in ppm.

	17A	17B	17C	17*
SiO_2	69.55	69.28	69.22	69.39 ± 0.17
Al_2O_3	16.08	15.90	15.90	15.99 ± 0.09
Fe_2O_{3T}	2.80	2.80	2.83	2.82 ± 0.02
MgO	0.63	0.70	0.73	0.68 ± 0.05
CaO	4.00	3.97	4.03	4.00 ± 0.03
Na_2O	4.00	4.46	4.29	4.23 ± 0.23
K_2O	2.47	2.42	2.54	2.48 ± 0.06
TiO_2	0.29	0.29	0.29	0.29 ± 0.00
MnO	0.04	0.05	0.04	0.05 ± 0.01
P_2O_5	0.13	0.13	0.12	0.13 ± 0.01
Ba	696	684	689	690 ± 6
Rb	41	41	38	40 ± 2
Sr	602	594	597	598 ± 4
Y	30	29	27	29 ± 2
Zr	171	171	168	170 ± 2
Nb	19	12	14	17 ± 3

One sample (17) was chosen to be run in triplicate to determine user error. Three fusion pellets and three pressed powder pellets (17A, 17B, and 17C) were made and analysed by XRF. Average values (17*) and errors were calculated. The results are tabulated in Table 3.1.2.

The purposes of the descriptive geochemistry were:

(i) to detect any compositional variations within the porphyritic units suggestive of bedding (i.e. cryptic layering)

(ii) to detect any chemical differences between the porphyritic units and the hypabyssal porphyries

(iii) to chemically classify the rocks.

3.2 Major Oxide Characteristics and Classification

Referring to Table 3.1.1 it can be seen that there is a systematic increase in CaO from bottom (N) to top (S) within the main porphyry unit (samples 15-23). This is the only oxide which shows regular variation, and it is most likely a reflection of the increase in carbonate alteration towards the Pipestone-Cameron Fault as noted in the field (see Section 2.1).

There are no significant differences between the intrusive porphyry (sample 28) and the upper porphyry, Unit 1, with the exception of K_2O content. A low value for K_2O (1.91 wt.%) is noted for the intrusive porphyry in comparison with the values obtained for the porphyry unit (2.48—4.00 wt.%).

Jensen (1975) proposed a cation percent plot for

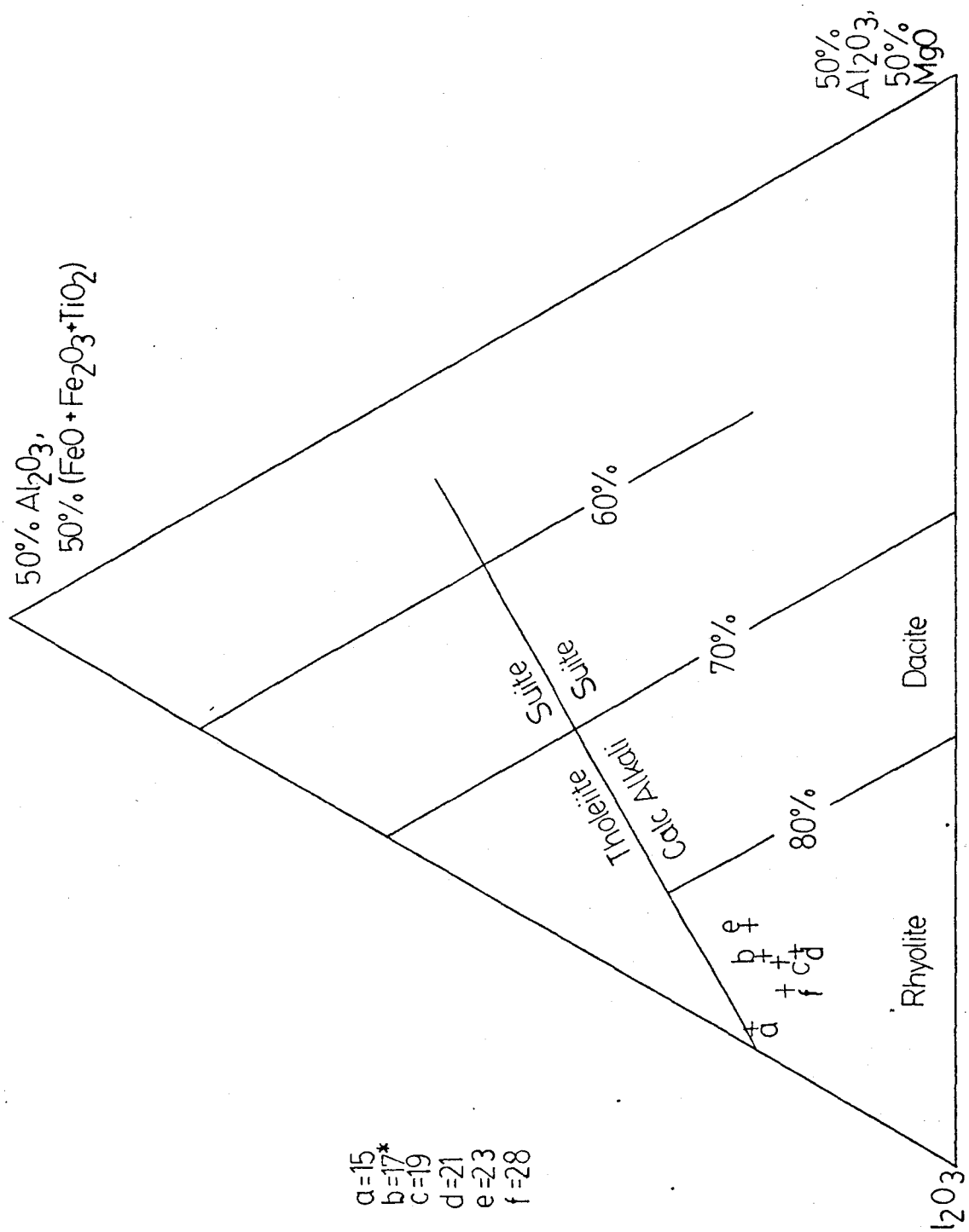

Figure 3.2 Jensen cation plot. Fields from Jensen(1975).

Al, Mg and Ti+total Fe to distinguish the calc-alkali and tholeiitic suites, and the various volcanic rock types. These particular cations show a low tendency for mobility and thus aren't greatly affected by metamorphic alteration. Consequently this plot has gained acceptance, especially for rocks of Archaean age. All six samples plot in the calc-alkali rhyolite field (see Figure 3.2).

Barth norms were calculated to give an indication of the mineralogy of the pre-altered rock. Results are tabulated in Table 3.2.

3.3 Trace Element Characteristics and Classification

Referring to Table 3.1.1, it can be seen that there is no systematic variation in trace elements from top to bottom in the upper porphyry (Unit 1).

Differences noted between the intrusive porphyry and the upper porphyry unit are the slightly higher Ba, Sr and Zr values and slightly lower Nb value of the porphyry intrusion.

Winchester and Floyd (1977) have constructed a series of grids for classifying volcanic rock types based upon their characteristic concentrations of Ti, Zr, Y, Nb, Ce, Ga, and Sc. These trace elements are immobile during alteration and metamorphism (Cann, 1970). Thus, they provide a method of recognising original volcanic rock types in metamorphosed or al-

Table 3.2 Barth norms calculated from XRF analysis. 15-23=porphyry Unit 1; 28=porphyry intrusion.

	15	17*	19	21	23	28
Quartz	41.68	41.02	43.10	43.16	43.86	46.31
Orthoclase	16.15	12.40	18.55	20.00	14.45	9.55
Albite	15.40	21.15	16.90	17.55	24.10	22.80
Anorthite	22.00	18.90	12.40	10.90	5.65	13.25
Magnetite	1.92	1.72	0.90	0.57	2.31	0.51
Ilmenite	0.60	0.58	0.60	0.50	0.62	0.58
Haematite	0.52	0.53	0.90	1.37	0.27	1.45
Apatite	0.37	0.34	0.40	0.40	0.45	0.27
Corundum	1.07	1.72	4.50	3.92	6.53	4.27
Enstatite	0.12	1.36	1.36	1.56	1.64	0.94
Total	99.83	99.72	99.91	99.93	99.88	99.93
$(\frac{An}{An+Ab})100$	59	47	42	38	19	37

tered rocks. Two of these plots are found in Figures 3.3.1 and 3.3.2. All six samples plotted in the rhyodacite-dacite fields on both grids.

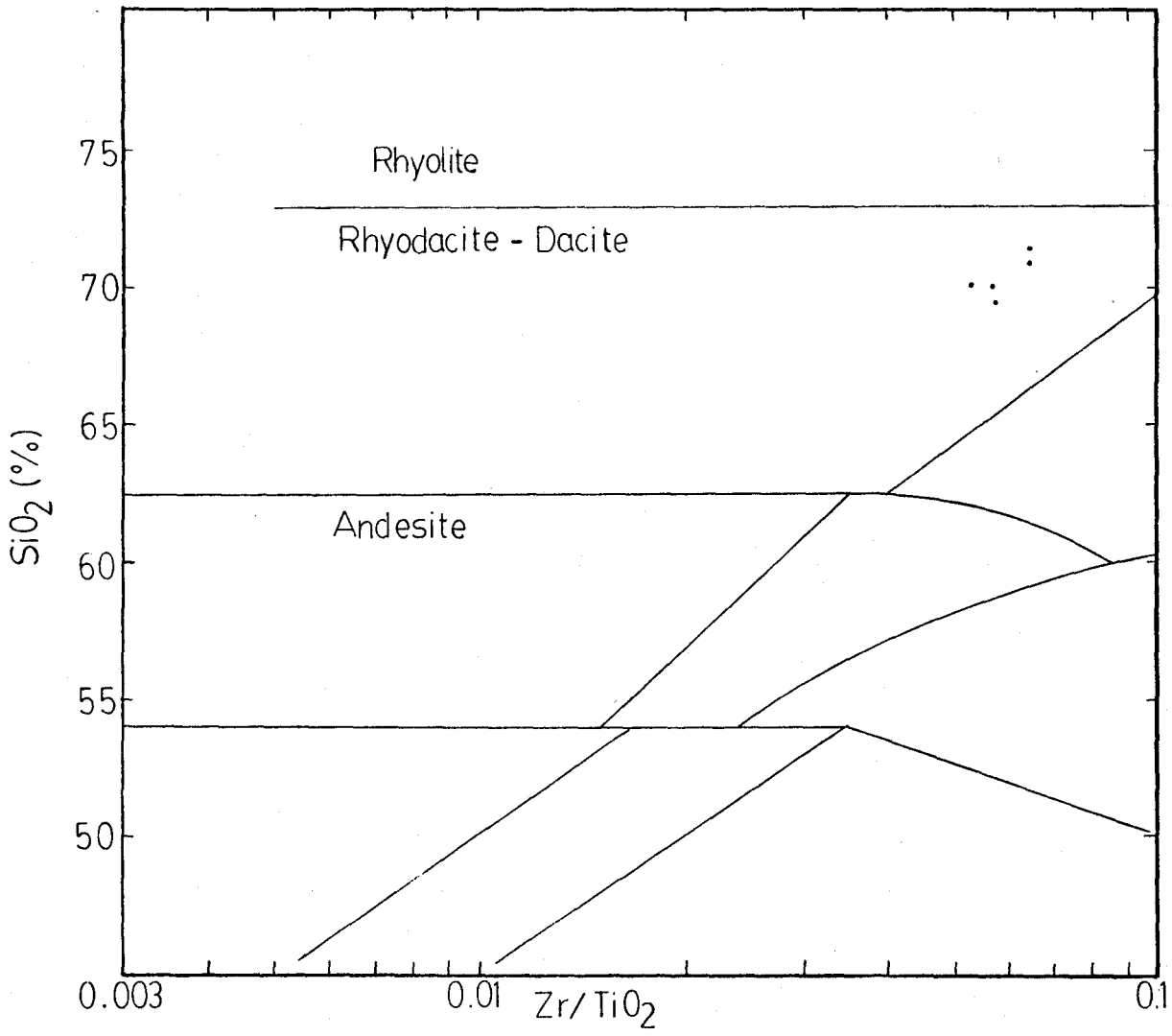

Figure 3.3.1 Zr/TiO_2—SiO_2 classification diagram. Fields from Winchester and Floyd[2] (1977).

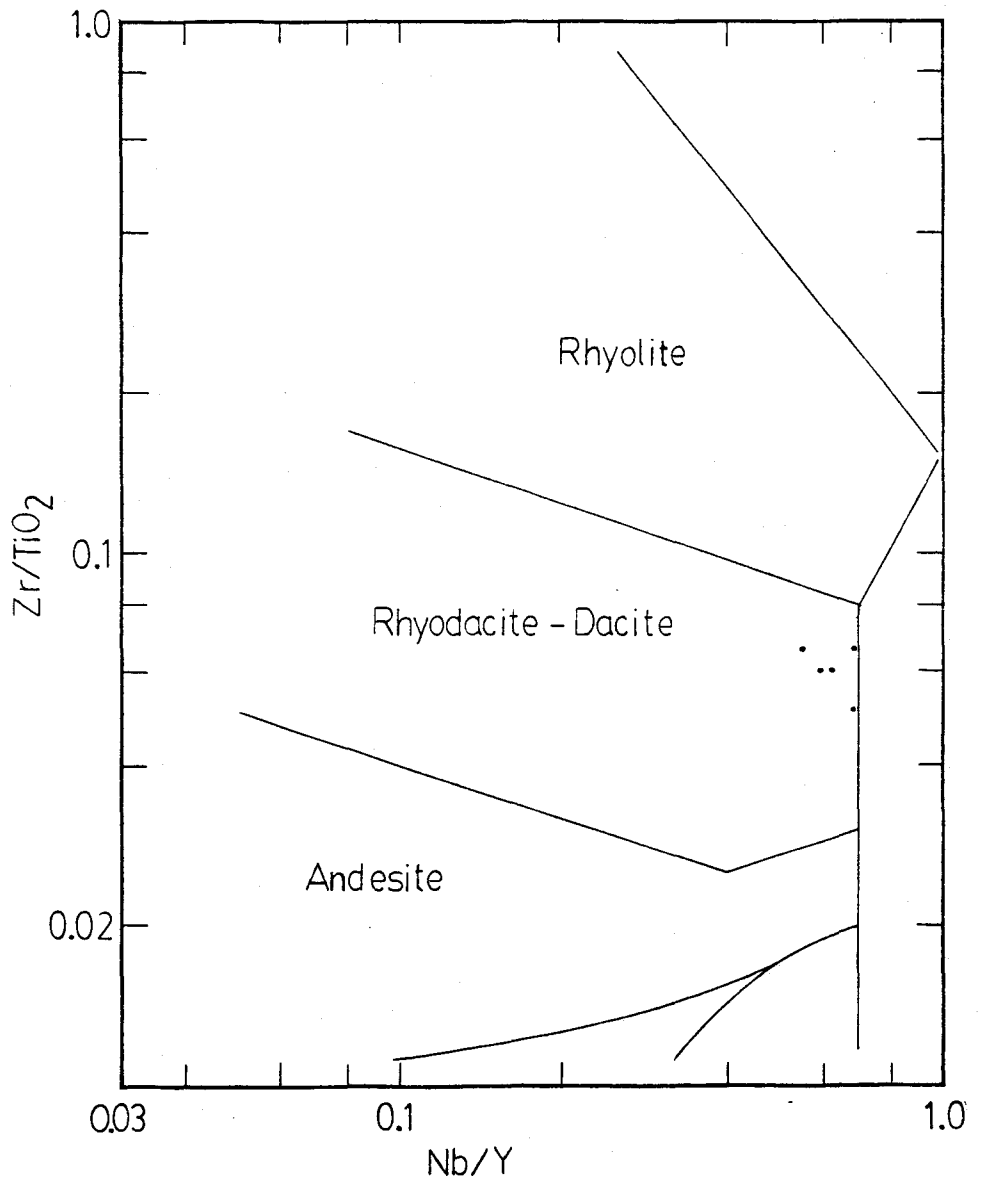

Figure 3.3.2 Nb/Y—Zr/TiO_2 classification diagram. Fields fron Winchester and Floyd (1977).

CHAPTER FOUR:

PETROGRAPHY

4.1 Porphyries

Thin sections were made from samples taken at 130 m intervals in a traverse perpendicular to strike across the porphyry Unit 1 described in Sections 1.2 and 2.1. This procedure was followed to determine whether there are any systematic variations within the unit. Also, since the unit is presently interpreted as an ash flow deposit, it was assumed that primary pyroclastic features such as glass shards, pumice or evidence of welding might be visible in thin section.

Table 4.1.1 gives the modal proportions of phenocrysts and matrix, based upon no less than 500 point counts per slide, and up to 1000 counts per slide. This was done to determine an accurate ratio of phenocrysts/matrix such that any increase or decrease within the unit could be noted.

The matrix was found to be very fine-grained, equigranular (0.01-0.02 mm), consisting predominantly of quartz, but also containing biotite, calcite, muscovite, plagioclase, chlorite and epidote in varying quantities. The amount of calcite decreases from top (sample 15) to bottom (sample 23) within the unit. Fine-grained mica laths within the matrix exhibit subparallel alignment.

Phenocrysts of both alkali and plagioclase feldspar, often broken and/or heavily altered, and containing in-

Table 4.1.1 Percent phenocrysts vs. matrix determined by point counts. 15-23=porphyry Unit 1; 25-28=porphyry intrusions.

Sample#	Quartz	Untwinned Feldspar	Plagioclase	Total Phenos	Matrix
15	5.5	5	7.5	18	82
17	2	5	9	16	84
19	5.5	2	3.5	11	89
19A	8.5	9	6	23.5	76.5
21	7.5	5	13	25.5	74.5
21A	12.5	3.5	12.5	28.5	71.5
23	8	5.5	7.5	21	79
25	8	7.5	11	26.5	73.5
26	12	9.5	10	31.5	68.5
28	6	10	10	26	74

PLATE 4.1

(A) Photomicrograph of porphyry Unit 1 (sample 15) -- two rounded quartz phenocrysts are extinct. Cross-polarised light (7 x).

(B) Photomicrograph of porphyry Unit 1 (sample 21A). Cross-polarised light (14 x).

(C) Photomicrograph of porphyry Unit 1 (sample 23). Cross-polarised light (14 x).

(D) Subhedral feldspar phenocryst in porphyry Unit 1 (sample 21) showing alteration. Cross-polarised light (64 x).

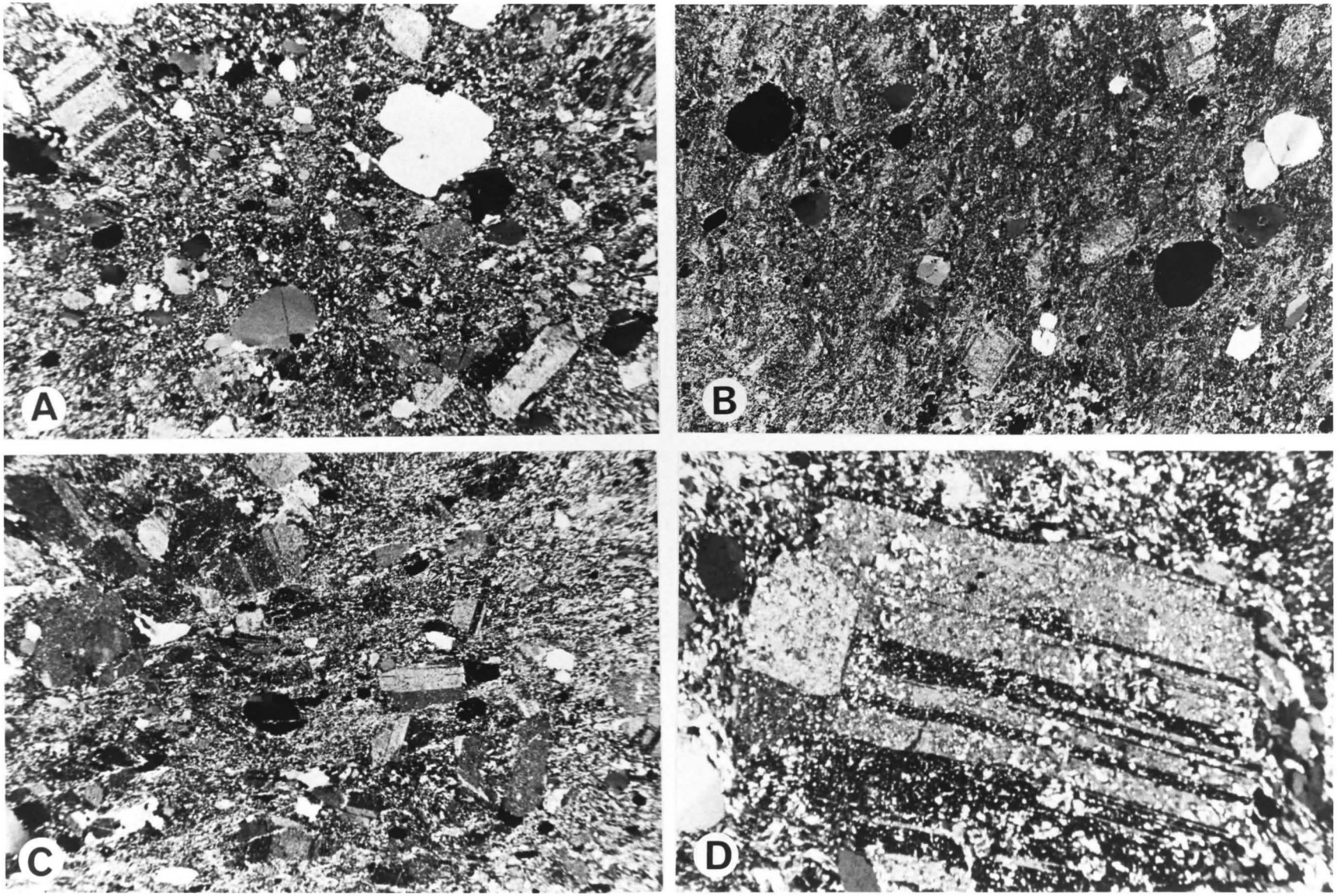
A
B
C
D

Table 4.1.2 Approximate matrix modes, estimated by eye from thin section. 05,33= ash fall tuff; 15-23=porphyry Unit 1; 25-28=porphyry intrusion.

Sample	Quartz	Biotite	Calcite	Muscovite	Plagioclase	Chlorite	Epidote	Opaques
05	59	20	10	1	5	5	--	--
33	64	20	5	minor	1	minor	10	--
15	45	--	30	20	5	minor	--	minor
17	55	minor	14	24	5	minor	2	minor
19	60	--	10	25	3	--	1	1
19A	65	1	5	25	2	1	--	1
21	55	minor	5	25	5	minor	--	--
21A	55	1	10	28	5	1	--	--
23	67	1	5	20	5	1	--	minor
25	78	1	--	15	5	--	--	1
26	78	1	--	17	4	--	2	1
28	73	2	--	20	5	--	--	minor

clusions of mica, are abundant (see Plate 4.1(D)). Alkali feldspar phenocrysts are most commonly anhedral. Plagioclase phenocrysts range from anhedral to subhedral, to rarely euhedral. Phenocrysts of quartz are also abundant, ranging from rounded grains (see Plate 4.1 (A)) to broken and/or strained crystals.

Crystal orientations are random. Crystal sizes vary, from a minimum of roughly 0.25 mm up to a maximum of 4 mm in diameter. Quartz phenocrysts are generally larger than feldspars. The amount and type of crystals vary but in a random fashion (i.e., unrelated to position within the mapped unit). The ratio of phenocrysts to matrix varies from sample to sample, but most show proportions of >20% phenocrysts.

These samples displayed no features which could be interpreted as pumice or glass shards. However, this may be due to the fact that recrystallisation of the matrix during low-grade regional metamorphism has obliterated all primary textures.

Table 4.1.2 lists approximate modal proportions of the matrix components (as estimated by eye).

4.2 Pyroclastics

Samples were collected for thin section from two outcrops of fine-grained quartz-feldspar tuff for comparison with the porphyry units under study (Section 4.1).

The matrix is coarser-grained than that of the por-

phyry described in the last section--roughly 0.05-0.1 mm. Phenocrysts are finer-grained in comparison with the porphyry unit, ranging from a minimum of about 0.25 mm to a maximum of about 1.5 mm.

Quartz is the most abundant matrix constituent. Biotite within the matrix defines a fair foiation (see Plate 4.2(A)). Minor amounts of chlorite may be associated with the biotite. Some larger (0.5 mm) flakes of muscovite are present. Epidote is abundant in one slide. Calcite is a major constituent as well.

Alakali feldspar phenocrysts are abundant, containing inclusions of mica. Plagioclase phenocrysts are less abundant. Feldspar phenocrysts in general due not show as great a degree fo alteration as those in the porphyry Unit 1. Quartz phenocrysts are common, and may display polycrystallinity and/or undulose extinction (see Plate 4.2(B)).

Table 4.1.2 lists approximate matrix modes.

4.3 Porphyry Intrusions

Samples were taken for thin section from two quartz-feldspar porphyry intrusions for comparison with the porphyry units under study (Section 4.1).

These intrusive porphyry samples are all similar in mineralogy and texture. The groundmass is fine-grained (0.05-0.1 mm) and is predominantly quartz. Coarser muscovite (1 mm maximum) is common. Biotite is rare, but

PLATE 4.2

Quartz phenocryst and biotite foliation in quartz-feldspar tuff (sample 33), 32 x.
(A) plane-polarised light
(B) cross-polarised light.

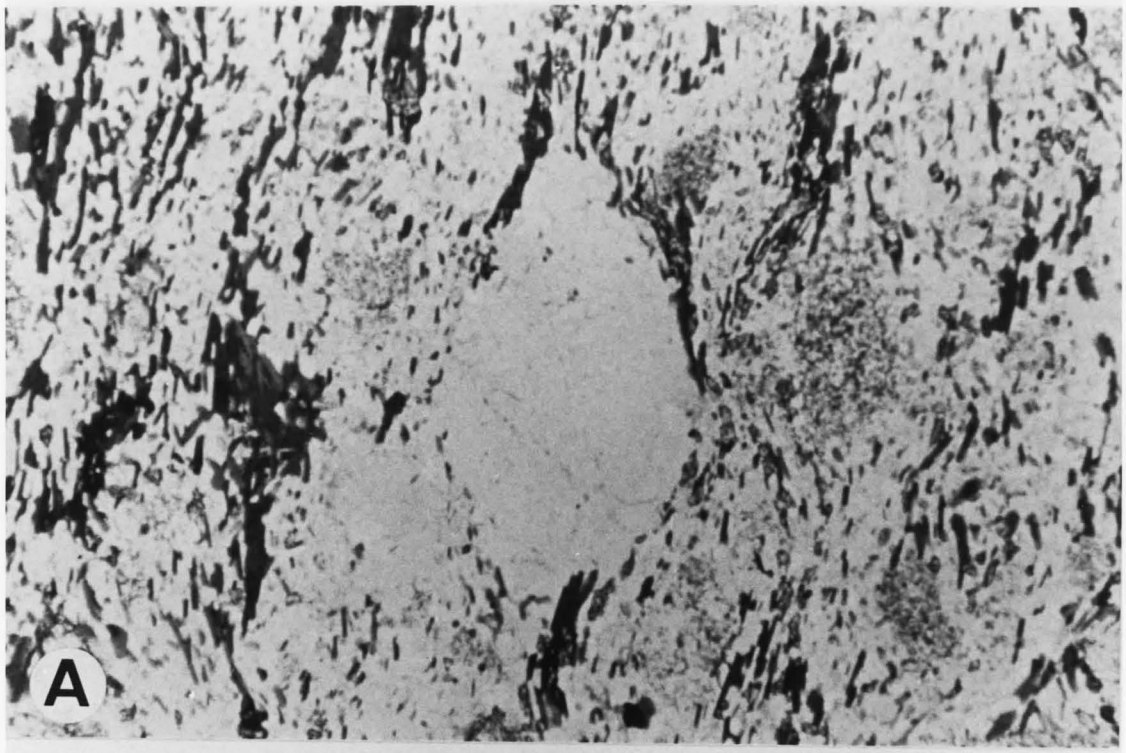
A

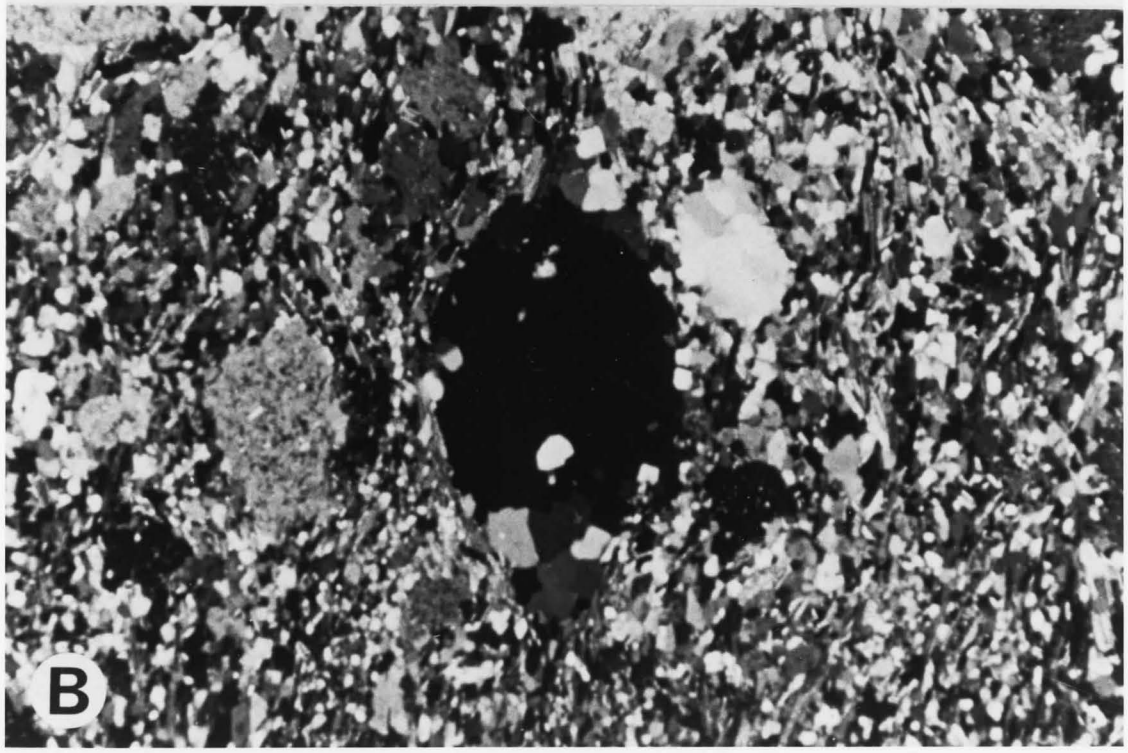
B

where present it exhibits subparallel orientation. Epidote may be present in very small amounts. Calcite is not present in any of these samples.

Medium to coarse (0.5-5 mm) phenocrysts of quartz and feldspar are abundant, slightly moreso than in the porphyry Unit 1 (see Figure 4.1.1). Quartz phenocrysts are polycrystalline, consisting of several crystals of roughly equant shape. Undulatory extinction is common (see Plate 4.3).

Alkali and plagioclase feldspars are present in roughly equal proportions. Crystals are generally anhedral and may contain inclusions of mica. As in the pyroclastics, the feldspars in these samples do not show the same degree of alteration as those in the porphyry unit.

Table 4.1.2 lists approximate matrix modes. Plate 4.4 compares matrix grain sizes of the intrusive porphyry (A), the porphyries under study (B) and the pyroclastics (C).

PLATE 4.3

Polycrystalline quartz phenocryst in porphyry intrusion (sample 28), 14 x.
(A) plane-polarised light
(B) cross-polarised light.

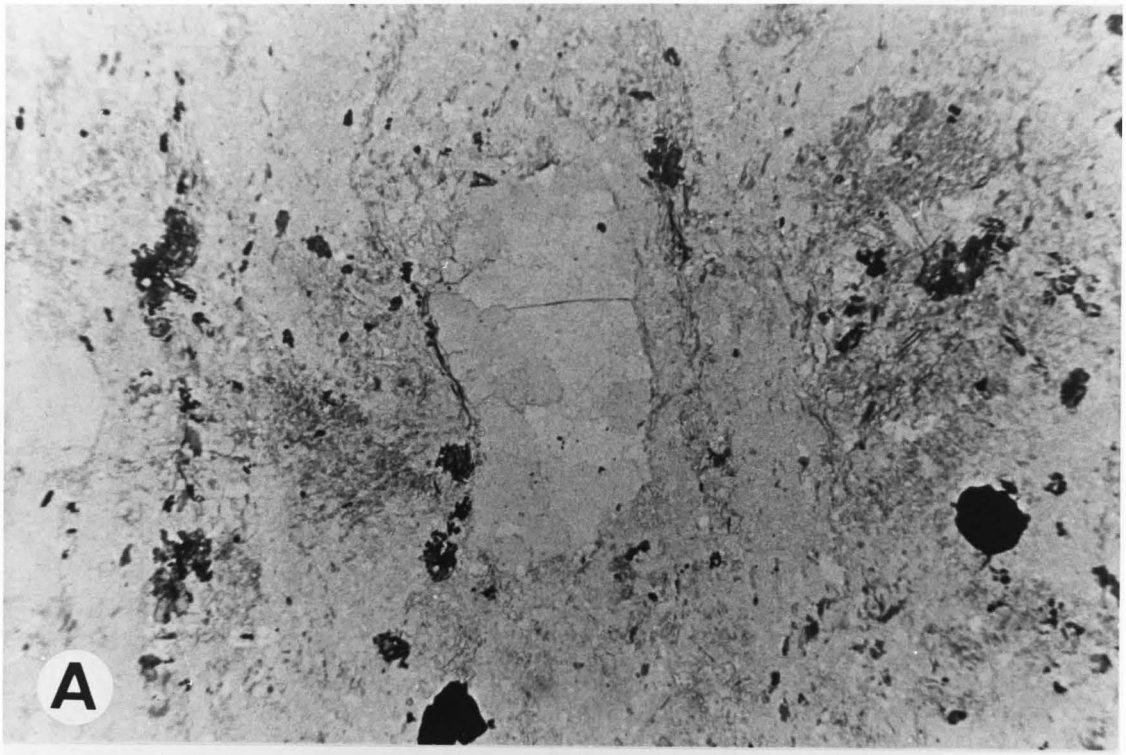
A

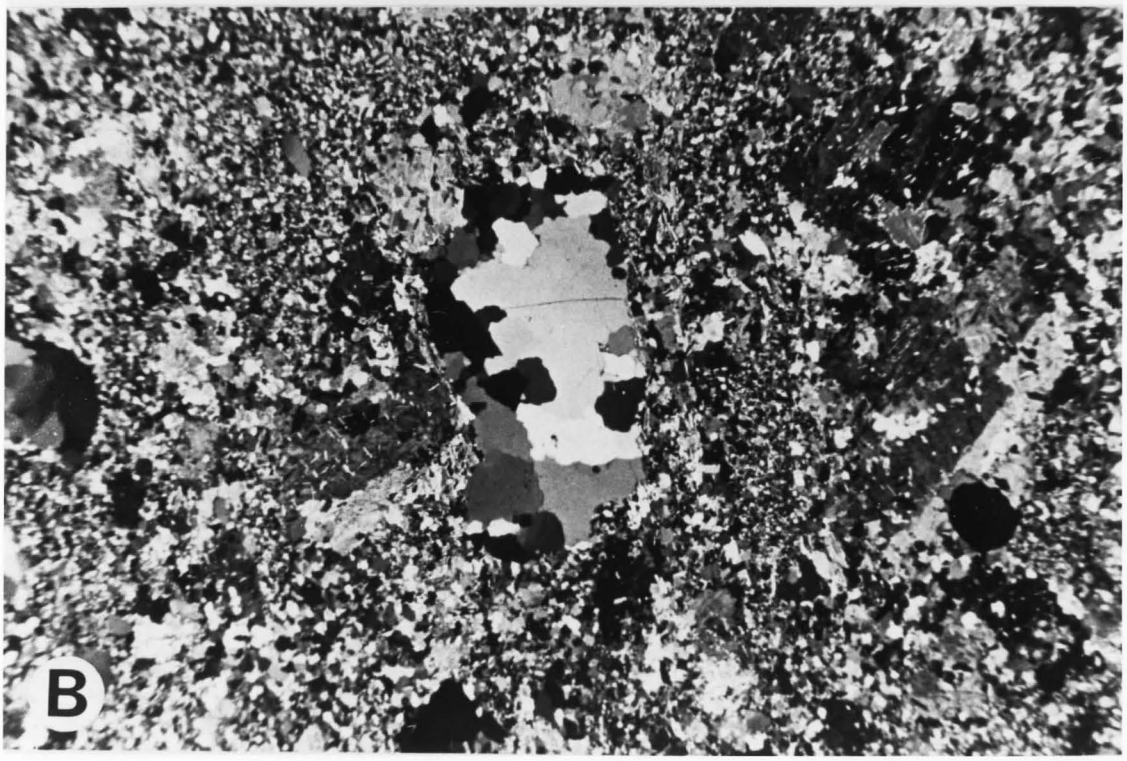
B

PLATE 4.4

Comparative matrix grain sizes. Cross-polarised light (40 x).

(A) Intrusive porphyry (sample 28)

(B) Porphyry Unit 1 (sample 17)

(C) Quartz-feldspar tuff (sample 33).

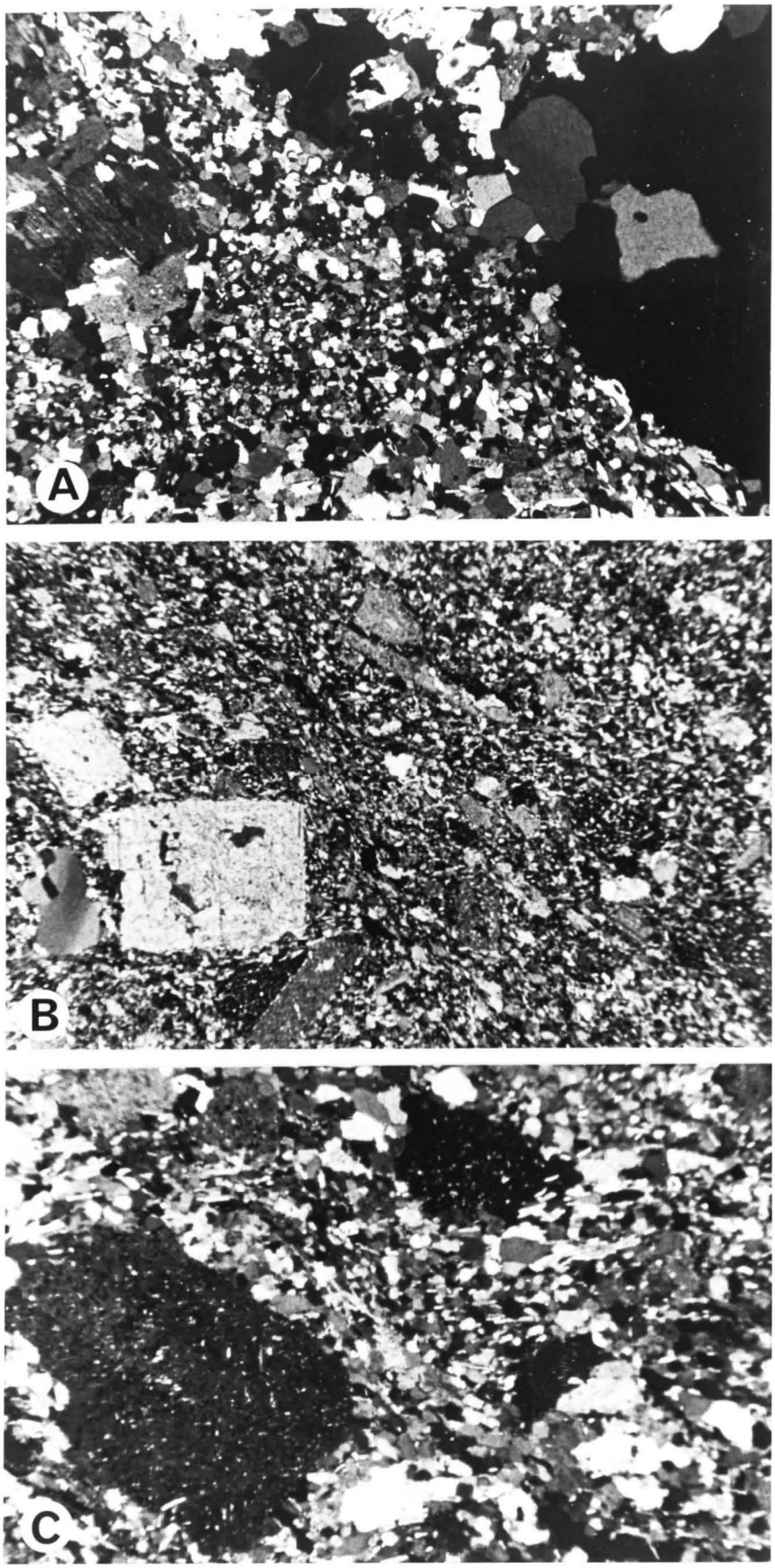
A
B
C

CHAPTER FIVE:

DISCUSSION AND CONCLUSIONS

The purpose of this thesis is to determine the method of emplacement of the porphyry units described in Sections 1.2, 2.1, and 4.1. Three possibilities are considered: (i) ash flow (ii) intrusion or (iii) lava flow.

(i) The present interpretation (Johns, in prep.) suggests that these units are ash flow deposits. For purposes of comparison with the porphyries under study, a description of ash flow tuffs, summarised from Fisher and Schminke (1984) is presented.

Ash flows are "volcanically produced hot, gaseous, particulate density currents" (Fisher and Schminke, p. 186) transported in glowing avalanches (nuées ardentes).

Ash flow tuff is composed primarily of ash-sized particles (50% by definition) which form a matrix to pumice or lithic lapilli. Glass shards are the most common ash-sized component; crystals are the second most common. They are often broken during eruption and transportation, and may range in abundance from 0 to 50%. Quartz, plagioclase and alkali feldspar are the most common phenocrysts, with minor amounts of biotite, iron-titanium oxides, and sphene.

Ash flow tuffs are often poorly sorted, massive and may be confined to topographic lows. They display evidence for being hot (i.e., welding). Many flow dep-

osits display a marked upward increase in crystals, as well as changes in mineral type and composition, and other chemical changes indicative of zoned parent magma chambers (an inverse stratigraphy is preserved in the tuffs).

Large trace element gradients are known from several Phanerozoic ash flow tuffs (Hildreth, 1979; Noble, et al., 1979; Mahood, 1981a, 1981b; Michael, 1983). Hildreth defined lower units as "Early" eruptive products and upper units as "Late". "Early" tuffs were found to be enriched in Rb, Y, Zr, Nb, Cs and the heavy rare earths, compared to "Late" tuffs. "Late" tuffs were reported as being enriched in Ba, Sr, Eu, and the light rare earths, as well as in the major elements Fe, Mg, Ti, Mn, Ca, and P.

Calc-alkali dacites and rhyolites are the most common compositions of large volume flow deposits.

(ii) The second possible origin for the porphyry units under study is by intrusion. Hypabyssals commonly occur in or near felsic volcanics in greenstone terrains. Hypabyssal activity may be contemporaneous with volcanic activity--dykes, sills and stocks occurring as subvolcanic intrusions. These tend to be fine-grained, porphyritic and generally felsic.

(iii) The third possible method of emplacement of the porphyry units is by surface lava flow. Ayres (1969) has listed the field characteristics of porphyritic

Table 5.1 Field criteria used in the greenschist facies, after Ayres (1969).

Felsic Metatuff

1. Abundant sand-size, lenticular felsic fragments.
2. Rare sand-size, lenticular mafic fragments.
3. Abundant angular, sand-size plagioclase.
4. Rare sand-size quartz.
5. Rare felsic metavolcanic lapilli.
6. Abundant, wispy, very fine-grained quartz-plagioclase-white mica matrix.

Porphyritic Felsic Flow

1. Sand-size rock fragments.
2. Rare metavolcanic lapilli.
3. Subhedral-euhedral, locally oriented, fine- to medium-grained plagioclase phenocrysts.
4. Rare fine- to medium-grained quartz phenocrysts.
5. Abundant very fine-grained quartz-plagioclase-white mica matrix, locally aphanitic.

felsic flows (Table 5.1). Felsic porphyry flows may contain rare foreign fragments such as rock fragments or metavolcanic lapilli. Locally oriented subhedral to euhedral, fine to medium-grained feldspar phenocrysts are common. Fine- to medium-grained phenocrysts of quartz are also found. Phenocrysts are set in an abundant aphanitic quartz-plagioclase-white mica matrix.

It is apparent that the porphyry units under study are similar, in some respects, to ash flow tuffs. That is, the porphyries do contain abundant crystals of quartz, plagioclase and alkali feldspar. They are composed primarily of ash-sized particles. The porphyries are geochemically similar in that they are calc-alkali rhyolites or rhyodacites.

However, no systematic change in crystal abundances was noted. No trace element gradients were found. Some enrichment of Ba and Sr (as well as Ca, as discussed in Section 3.2) was observed at the top of the unit (sample 15) in comparison with the base (sample 23) but these enrichments are not systematic, as would be expected. It should be noted that not all volcanic rocks are produced from zoned magma chambers. Therefore, the absence of chemical zonation does not preclude an ash flow emplacement model.

The porphyries show neither pumice nor lithic lapilli nor glass shards in either the field or in thin section. Although rocks of Precambrian age which have

retained evidence of welded-tuff origin are known (Ross and Smith, 1961) they are exceptional. The thesis area has undergone lower greenschist metamorphism, recrystallisation and intense shearing and alteration. These processes would have destroyed any primary pyroclastic features had they been present.

There are no significant differences between the porphyry unit under study and the intrusive porphyry in terms of major or trace elements.

Due to the poor exposure of the field area no contacts were observed. However, the are no changes in the porphyry or surrounding pyroclastics, where outcrops were found in close proximity, to suggest chilled or baked margins.

The porphyry unit shows a finer-grained matrix than the intrusion. The porphyry unit, being so much larger than the porphyry intrusion (at present erosional surface), would be expected to have a much coarser matrix if it was an intrusion (a larger body takes longer to cool and therefore has longer to crystallise).

No foreign fragments were observed within the porphyry units. Crudely oriented subhedral feldspars were noted at two locations. Phenocrysts of both feldspar and quartz are common, set in a very fine-grained quartz-plagioclase-mica matrix. The finer grain size (as compared to the tuffs or the intrusive porphyry) of the porphyry unit may be indicative of rapid cooling, more

characteristic of a surface lava flow (or flows).

CONCLUSION

Lack of convincing evidence in support of either of the first two hypotheses, namely those of ash flow or intrusive emplacements, and with little evidence against the third hypothesis, the author is left to conclude that these porphyritic units are most probably felsic porphyritic flows.

REFERENCES CITED

Ayres, L.D.

1969: Geology of the Muskrat Dam Lake Area; Ontario Division of Mines, Geological Report 74.

Blackburn, C.E.

1981: Kenora-Fort Frances Sheet, Kenora, Rainy River Districts; Ontario Geological Survey, Map 2443, Geological Compilation Series, 1973-1978.

Burwash, E.M.

1934: Geology of the Kakagi Lake Area; Ontario Division of Mines, 1933 Annual Report, V42(4), p.41-92.

Cann, J.R.

1970: Rb, Sr, Y, Zr and Nb in some ocean floor basaltic rocks; Earth and Planetary Science Letters, 10, p. 7-11.

Davis, D.W., and Edwards, G.R.

1982: Zircon U-Pb ages from the Kakagi Lake Area, Wabigoon Subprovince, NW Ontario; Canadian Journal of Earth Sciences, V19, p.1235-1245.

Fisher, R.V.

1966: Rocks composed of volcanic fragments and their classification; Earth Science Reviews, V1,p.287-298.

Fisher, R.V.,and Schminke, H-U

1984: Pyroclastic Rocks; Springer-Verlag, New York.

Hildreth, W.

1979: Bishop Tuff: Evidence for origin of compositional zonation; in Ash Flow Tuffs, Geological Society of America Special Paper 180.

Jensen, L.S.

1976: A new cation plot for classif ying sub-alkalic volcanic rocks; Ontario Division of Mines, Miscellaneous Paper 66.

Johns, G.W., and Davison, J.G.

1983a: Precambrian Geology of the Long Bay-Lobstick Bay Area, Western Part, Kenora District;

Ontario Geological Survey Map P.2594, Geological Series-Preliminary Map; scale 1:15 840. Geology 1982.

1983b: Precambrian Geology of the Long Bay-Lobstick Bay Area, Eastern Part, Kenora District; Ontario Geological Survey Map P.2595, Geological Series-Preliminary Map; scale 1:15 840. Geology 1982.

Mahood, G.A.

1981a: A summary of the geology and petrology of the Sierra La Primavera, Jalisco, Mexico; Journal of Geophysical Research, 86(B11), p. 10 137 - 10 152,

1981b: Chemical evolution of a Pleistocene rhyolitic center: Sierra La Primavera, Jalisco, Mexico; Contributions to Mineralogy and Petrology, 77, p.129-149

Marchand,M.

1973: Determination of Rb, Sr and Rb/Sr by XRF; Technical Memo 73-2, Department of Geology, McMaster University, Hamilton, Ontario.

Michael, P.J.

1983: Chemical differentiation of the Bishop Tuff; Geology, 11(1), p.31-34.

Moorhouse, W.W.

1965: Stratigraphic position of sulphides in the Archaean; Transcripts of the Canadian Institute of Mining and Metallurgy, V58, p.947-959.

Noble, D.C., Rigot, W.L., and Bowman, H.R.

1979: Rare earth element content of some highly differentiated ash flow tuffs; in Ash Flow Tuffs, Geological Society of America, Special Paper 180.

Ross, C.S., and Smith, R.L.

1961: Ash-Flow Tuffs: Their Origin, Geologic Relations, and Identification; United States Geological Survey, Professional Paper 366.

Schmid, R.

1981: Descriptive nomenclature and classification of pyroclastic deposits and fragments: Recommendations of the IUGS Subcommission on the Systematics of Igneous Rocks; Geology, V9, p.41-43.

Stockwell, C.H., McGlynn, J.C., Emslie, R.F., Sanford, B.V., Norris, A.W., Donaldson, J.A., Fahrig, W.F., and Currie, K.L.

1970: Geology of the Canadian Shield; in Geology and Economic Minerals of Canada, R.J.W. Douglas (Sci. Ed.), Geological Survey of Canada, Economic Geology Report 1.

Trowell, N.F., Blackburn, C.E., and Edwards, G.R.

1980: Preliminary Geological Synthesis of the Savant Lake-Crow Lake Metavolcanic-Metasedimentary Belt, N.W. Ontario; Ontario Geological Survey Miscellaneous Paper 89.

Winchester, J.A., and Floyd, P.A.

1977: Geochemical discrimination of different magma series and their differentiation products using immobile elements; Chemical Geology, 20, p.325-343.

In Preparation

Easton, R.M., and Johns, G.W.

Volcanology and Mineral Exploration: The Application of Physical Volcanology and Facies Studies.

Johns, G.W.

Geology of the Long Bay-Lobstick Bay Area, Lake of the Woods, District of Kenora; Ontario Geological Survey, Open File Report.